Numerical Modelling of an Alaska 1964-type Tsunami at the Canadian Coast Guard Base in Seal Cove, British Columbia

Isaac V. Fine, Richard E. Thomson, Lauren M. Lupton and Stephen Mundschutz

Ocean Sciences Division

Fisheries and Oceans Canada

Institute of Ocean Sciences

9860 West Saanich Road

Sidney, BC

V8L 4B2

2018

Canadian Technical Report of Hydrography and Ocean Sciences 321

Fisheries and Oceans Canada | Pêches et Océans Canada

Canada

Canadian Technical Report of Hydrography and Ocean Sciences

Technical reports contain scientific and technical information of a type that represents a contribution to existing knowledge but which is not normally found in the primary literature. The subject matter is generally related to programs and interests of the Oceans and Science sectors of Fisheries and Oceans Canada.

Technical reports may be cited as full publications. The correct citation appears above the abstract of each report. Each report is abstracted in the data base *Aquatic Sciences and Fisheries Abstracts.*

Technical reports are produced regionally but are numbered nationally. Requests for individual reports will be filled by the issuing establishment listed on the front cover and title page.

Regional and headquarters establishments of Ocean Science and Surveys ceased publication of their various report series as of December 1981. A complete listing of these publications and the last number issued under each title are published in the *Canadian Journal of Fisheries and Aquatic Sciences*, Volume 38: Index to Publications 1981. The current series began with Report Number 1 in January 1982.

Rapport technique canadien sur l'hydrographie et les sciences océaniques

Les rapports techniques contiennent des renseignements scientifiques et techniques qui constituent une contribution aux connaissances actuelles mais que l'on ne trouve pas normalement dans les revues scientifiques. Le sujet est généralement rattaché aux programmes et intérêts des secteurs des Océans et des Sciences de Pêches et Océans Canada.

Les rapports techniques peuvent être cités comme des publications à part entière. Le titre exact figure au-dessus du résumé de chaque rapport. Les rapports techniques sont résumés dans la base de données *Résumés des sciences aquatiques et halieutiques.*

Les rapports techniques sont produits à l'échelon régional, mais numérotés à l'échelon national. Les demandes de rapports seront satisfaites par l'établissement auteur dont le nom figure sur la couverture et la page de titre.

Les établissements de l'ancien secteur des Sciences et Levés océaniques dans les régions et à l'administration centrale ont cessé de publier leurs diverses séries de rapports en décembre 1981. Vous trouverez dans l'index des publications du volume 38 du *Journal canadien des sciences halieutiques et aquatiques*, la liste de ces publications ainsi que le dernier numéro paru dans chaque catégorie. La nouvelle série a commencé avec la publication du rapport numéro 1 en janvier 1982.

Canadian Technical Report of
Hydrography and Ocean Sciences 321

2018

NUMERICAL MODELLING OF AN ALASKA 1964-TYPE TSUNAMI AT THE CANADIAN COAST GUARD BASE IN SEAL COVE, BRITISH COLUMBIA

by

Isaac V. Fine, Richard E. Thomson, Lauren M. Lupton and Stephen Mundschutz

Ocean Sciences Division
Fisheries and Oceans Canada
Institute of Ocean Sciences
9860 West Saanich Road
Sidney, BC, V8L

© Her Majesty the Queen in Right of Canada, 2018.

Cat. No. Fs97-18/321E-PDF ISBN 978-0-660-24928-5 ISSN 1488-5417

Correct citation for this publication:

Isaac V. Fine, Richard E. Thomson, Lauren M. Lupton and Stephen Mundschutz 2018. Numerical Modelling of an Alaska 1964-type Tsunami at the Canadian Coast Guard Base in Seal Cove, British Columbia. Can. Tech. Rep. Hydrogr. Ocean Sci. 321: v + 33p.

Contents

1 THE GREAT ALASKA 1964 EARTHQUAKE AND TSUNAMI 1

2 NUMERICAL SIMULATION OF THE 1964 TSUNAMI 3

2.1 Model Setup: Nested Grid Formulation 3

2.1.1 Coarse Grid (Grid 1) 4

2.1.2 Intermediate Grid (Grid 2) 5

2.1.3 Intermediate Grid (Grid 3) 8

2.1.4 Final Grid (Grid 4) 9

2.2 Model Reference Levels 10

2.3 The Tsunami Source Distribution 10

3 RESULTS 13

3.1 Comparison of Modelled Tsunami Waves with Observed Waves at the Prince Rupert Tide Gauge 13

3.2 Maximum Tsunami Heights 14

3.3 Detailed Results for Seal Cove: Variations in Sea Level and Tsunami-Induced Currents 18

4 CONCLUSIONS 27

5 ACKNOWLEDGEMENTS 29

6 REFERENCES 31

ABSTRACT

Numerical Modelling of an Alaska 1964-type Tsunami at the Canadian Coast Guard Base in Seal Cove, British Columbia.

Isaac V. Fine, Richard E. Thomson, Lauren M. Lupton and Stephen Mundschutz 2018. Numerical Modelling of an Alaska 1964-type Tsunami at the Canadian Coast Guard Base in Seal Cove, British Columbia. Can. Tech. Rep. Hydrogr. Ocean Sci. 321: v + 33p.

The magnitude 9.2 earthquake that occurred off the coast of Alaska in March 1964 generated large tsunami waves that were responsible for considerable destruction along the west coast of Canada and the United States.

This work uses a nested-grid numerical tsunami model and an updated three-dimensional viscoelastic model of the 1964 earthquake, combined with a coseismic after-slip model of the Alaska rupture zone, to predict future extreme tsunami waves and currents at Seal Cove. The analysis is in anticipation of upgrades and modernization of the Coast Guard facility at the site.

Tsunami wave amplitudes at Seal Cove from a 1964-type event will reach 1.55 m above the tidal level. The second wave will be the highest, arriving about 100 minutes after the first wave crest. Wave induced currents at Seal Cove will be weak but reach speeds of around 2.5 m/s (5 knots) in adjacent Fern Passage. Incorporation of a 50% safety factor indicates that the safe water level for Seal Cove should be at least 2.28 m above Mean Higher High Water, or 4.6 m above Mean Sea Level.

RESUME

Modélisation numérique d'un tsunami de type Alaska 1964 à la base de la Garde côtière canadienne à Seal Cove, en Colombie-Britannique.

Isaac V. Fine, Richard E. Thomson, Lauren M. Lupton and Stephen Mundschutz 2018. Numerical Modelling of an Alaska 1964-type Tsunami at the Canadian Coast Guard Base in Seal Cove, British Columbia. Can. Tech. Rep. Hydrogr. Ocean Sci. 321: v + 33p.

Le tremblement de terre d'une magnitude de 9,2 qui s'est produit au large de l'Alaska en mars 1964 a généré d'importantes vagues de tsunamis qui ont entraîné une destruction de taille le long de la côte ouest du Canada et des États-Unis.

Ce projet utilise un modèle de tsunami numérique à grille à maille variable et une nouvelle version du modèle viscoélastique tridimensionnel du tremblement de terre de 1964, combinés avec un modèle d'après glissement cosismique de la zone de rupture de l'Alaska, pour prévoir les vagues de tsunami extrêmes et les courants à venir à Seal Cove. L'analyse est effectuée dans le cadre des initiatives futures de mise à niveau et de modernisation de l'installation de la Garde côtière sur ce site.

À Seal Cove, l'amplitude de vagues de tsunami provoquées par un événement de type 1964 atteindrait 1,55 m au-dessus du niveau de marée. La deuxième vague serait la plus haute, frappant environ 100 minutes après la crête de la première vague. À Seal Cove, les courants engendrés par les vagues ne seraient pas très puissants, mais atteindraient des vitesses d'environ 2,5 m/s (5 nœuds) dans le passage Fern adjacent. La mise en œuvre d'un coefficient de sécurité de 50 % indique que le niveau d'eau sécuritaire de Seal Cove devrait se trouver au moins à 2,28 m au-dessus de la moyenne des pleines mers supérieures, ou 4,6 m au-dessus du niveau moyen de la mer.

Photo of Ocean Pacific Air at Seal Cove, BC, submitted by traveller Wim V (Sep 2017)

1 THE GREAT ALASKA 1964 EARTHQUAKE AND TSUNAMI

The second strongest instrumentally recorded earthquake in the World Ocean (moment magnitude, M_w=9.2) occurred off Alaska on March 28, 1964. The event generated a catastrophic tsunami, the second strongest in the 20th century after the 1960 Chilean tsunami, with maximum wave heights of 20 m near the earthquake source region. A large number of landslides and submarine landslides were also initiated, resulting in local tsunami waves as high as 70 m (Lander, 1996). The earthquake, which was the strongest instrumentally recorded earthquake in the North Pacific, occurred in the vicinity of Prince William Sound, leading to the widely used name of the "*Prince William Sound Earthquake*" (Spaeth and Berkman, 1967). Because of the event date (28 March 1964), the earthquake and associated Pacific-wide tsunami are also called the "*Good Friday Earthquake and Tsunami*".

The Good Friday tsunami was responsible for close to 130 deaths and about a million dollars in damage in Alaska, Washington, California and Hawaii (Spaeth and Berkman, 1967;

Lander, 1996; Stephenson *et al.*, 2007). Several locations on the coast of British Columbia suffered major damage (Clague *et al.*, 2003; Anderson and Gow, 2004; Stephenson *et al.*, 2007). The highest wave ever recorded in Canada occurred during this event at Shields Bay on the west coast of Graham Island (Haida Gwaii), where a wave crest was reported to be 5.2 m above the spring high water, or 9.8 m above the tidal datum. Most of the damage from the tsunami occurred in Port Alberni, where a wave reached 4.2 m above spring tide high water (Dunbar *et al.*, 1991; Fine *et al.*, 2008).

Several numerical models were constructed to simulate tsunami wave propagation from the 1964 event in the northeast Pacific Ocean (cf. Dunbar *et al.*, 1991; Myers and Baptista, 2001). Although these studies were able to simulate the main features of the tsunami impact on the British Columbia coast, a more detailed analysis based on high-resolution bathymetry and a more refined high-resolution source region of the uplift distribution is needed. Because of its exceptional characteristics, the 1964 Alaska tsunami is typically considered as a proxy for a major future tsunami along the Pacific coast of North America (Suleimani *et al.*, 2013).

The purpose of this report is to present results for numerically simulated tsunami waves generated by an Alaska 1964-type earthquake with moment magnitude $M_w \sim 9.2$. Focus is on the expected tsunami waves for the Canadian Coast Guard Station at Seal Cove, British Columbia. This research is part of a larger study to inform future redesigns of Coast Guard stations to mitigate the impact on the operability of these stations following a major disaster.

2 NUMERICAL SIMULATION OF THE 1964 TSUNAMI

2.1 MODEL SETUP: NESTED GRID FORMULATION

Accurate numerical simulation of tsunami waves in the rapidly shoaling regions of the west coast of British Columbia requires setting up the model domain as a series of nested grids of ever finer spatial and temporal resolution. The use of nested grids of smaller cell dimensions and time steps makes it possible to resolve tsunami wave configurations as they propagate into the shallow coastal regions. The principal requirements for numerical models using nested grids are as follows:

- Nested grid cell sizes are generally obtained by dividing the initial, large-scale coarse numerical grid by an integer, typically 3 to 5. Integers larger than this can lead to grid interface problems;
- Nested grids are needed in near-coastal areas; the coarse "parent" grid should be of sufficient extent to resolve possible feed-back effects that the nested grid may have on the parent grid during the simulation time;
- A good interface between the inner and outer domains is required to avoid errors and model instability associated with point matching between the different grids. This should allow two-way fluxes without trapping shorter waves at the inner domain boundaries;
- High resolution bathymetry, external forcing and observations are needed for model domain setup, initialization and validation at each domain level; here the nested-grid formulation is similar to that used in well-known tsunami models, TUNAMI and COMCOT (Liu *et al.*, 1998; Imamura, *et al.*, 2006; Wang, 2009).

Dispersion effects can be included in the model by substituting numerical dispersion for the actual physical dispersion. Solving this issue (see for example, Imamura et al., 1988) has made it possible for investigators to cover large, open ocean regions, representative of an area affected by a 1964 style tsunami, using a relatively coarse grid with a cell size of roughly 10 km by 10 km (4-5 arc-seconds).

Because of the relatively long periods of the tsunamis generated in the deep water source regions used in this study, and because of the relatively short propagation times of 2-3 hours between the source region and the Seal Cove site, the dispersion effect is negligible. In this case, high bathymetric resolution is the important factor for modelling wave propagation in the offshore regions.

To achieve this the present project uses a series of four nested grids for the Alaska 1964 tsunami model (Table 1). The choice of model grids takes into account the need for high spatial resolution to accurately resolve the reflection and transformation of the waves and the need for a sufficiently large spatial extent to capture the effects of frequency dispersion during long distance wave propagation.

Table 1: Parameters of the numerical grids used in the Alaska 1964 tsunami generation and propagation model. Grid extent is along the *x* (eastward) and *y* (northward) coordinate directions and is presented in degrees (°). Numerical grid cell sizes for Grids 2, 3 and 4 are roughly 270, 54 and 11 m, respectively. CHS refers to the Canadian Hydrographic Service.

Grid No.	Extent (*x*, *y*) (degrees)	Array (number of grid points)	Cell size (*x*, *y*) (degrees)	Source of data	Processing type
1	35.0, 17.0	1401, 1361	0.025, 0.0125	GEBCO 2014 30 arc- seconds gridded data	Filtering and bilinear interpolation
2	5.0, 6.2	1201, 2480	0.00416667, 0.0025	BC Coastal Relief, 3 sec, Southern Alaska Coastal Relief 8 sec	Filtering and bilinear interpolation
3	1.0086, 0.526	1339, 1053	0.0008333, 0.0005	CHS bathymetry data	Filtering and bilinear interpolation
4	0.13, 0.06	781, 701	0.000166667, 0.0000833	CHS bathymetry data, coast line, chart	Kriging, smoothing, bilinear interpolation

2.1.1 Coarse Grid (Grid 1)

Grid 1 is the outer domain and covers the northeast Pacific, encompassing the major source region used in the simulations, the Alaska Failure Zone (Figure 2.1). We note that the northeast Pacific is an important tsunami wave generation region through which all offshore tsunamis propagate on their way to the British Columbia coast. The spatial resolution of the coarse grid is 90 arc-seconds in the east-west direction (spatial scales in x range from 1.4 km to

2.2 km, depending on latitude) and 45 arc-seconds in the north-south direction (1.4 km grid size in the *y*-direction). The grid is bounded by 45– 62°N, 157 – 122°W and was created using the 30 arc-second global bathymetry dataset GEBCO (Becker et al., 2009).

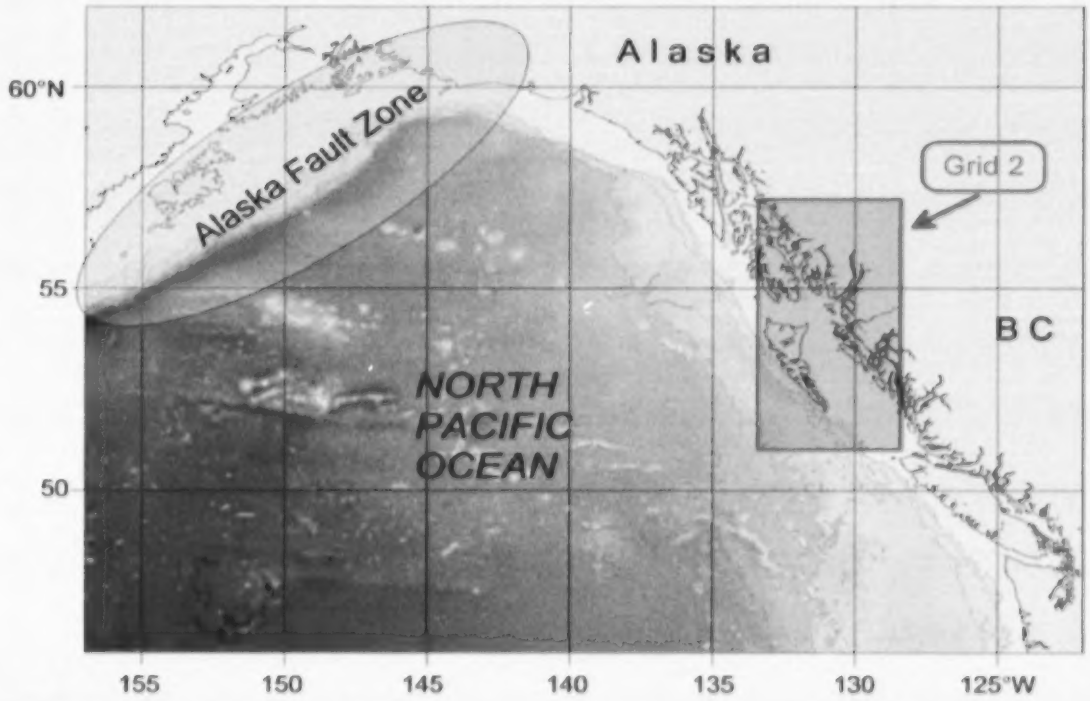

Figure 2.1. The region covered by the large-scale coarse grid numerical model for the northeast Pacific (Grid 1). Also shown is the Alaska Fault Zone that could generate tsunamis that impact the DFO Coast Guard facility. The insert shows the location of the first nested grid (Grid 2), covering the northwest coast of British Columbia.

2.1.2 Intermediate Grid (Grid 2)

Grid 2 covers northwest British Columbia and southeast Alaska (Figure 2.2). The location and coverage of the grid was chosen so that it extends equally north and south of the Prince Rupert region. This intermediate grid enables simulation of wave shoaling and wave transformation as the tsunami propagates from the deep ocean to the shelf and into coastal areas. The grid is also important for energy exchange between different parts of the coast and shelf areas.

The southern part of the grid was created using the British Columbia 3 arc-second Digital Elevation Model (NOAA, 2017); the northern part was created using the 8 arc-second Southern Alaska Coastal Relief (Candwell et al., 2012). The British Columbia coastal relief map stops at 54.20°N at its northern boundary and it does not include the Prince Rupert area. In contrast, the Alaska topographic relief map extends to 19°N and includes the Prince Rupert area, but does not have sufficient accuracy for the Canadian region and were excluded where the grid crossed into Canadian waters.

The excluded data were replaced with available Canadian Hydrographic Survey (CHS) data. Thus, the northern boundary between the datasets was at around 54.5°N in the northern part of Dixon Entrance. To ensure there were no discontinuities between the two datasets, a smooth transition zone was inserted between them. Grid 2 has a resolution of 15 arc-seconds in the east-west direction and 9 arc-seconds in the north-south direction, corresponding to spatial scales of approximately 270 m by 280 m, respectively (Table 1). The grid spans the northern coast with boundaries of 51°– 57°N, 134° – 128°W.

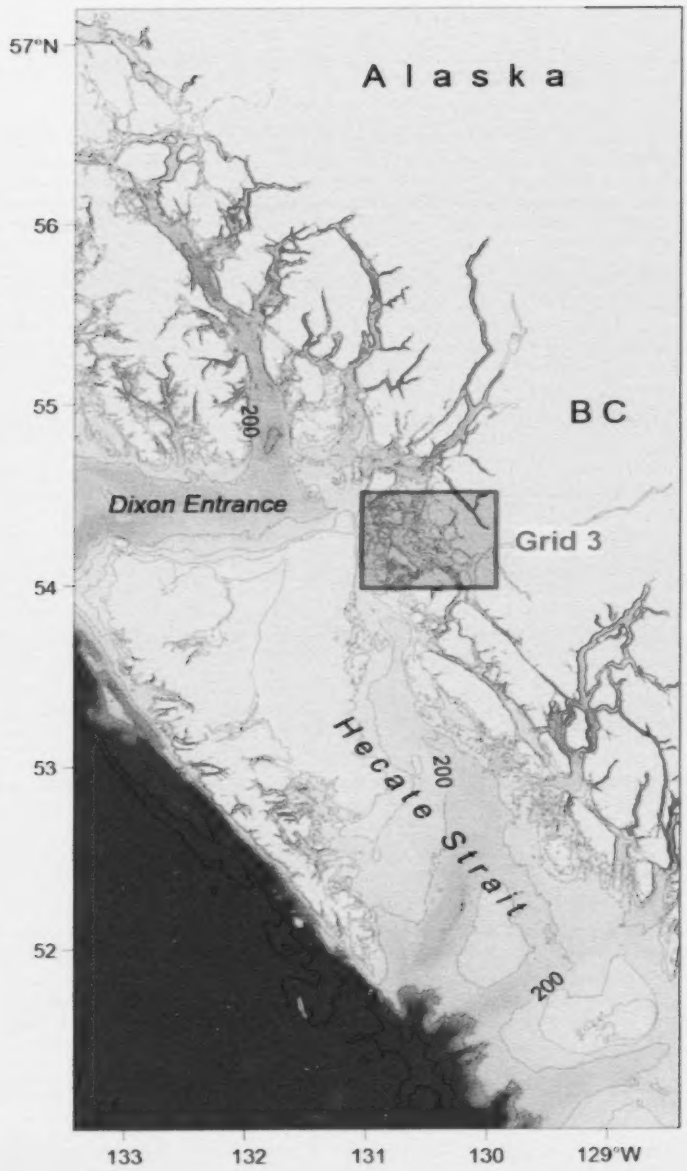

Figure 2.2. The region covered by the medium-scale bathymetric grid (Grid 2) for the northwest coast of British Columbia. The horizontal (x, y) grid cell scales for this region are approximately 270 m by 280 m, respectively. The insert shows the boundaries and location of the second nested grid (Grid 3) covering the region of Prince Rupert and Seal Cove. Depths are in metres (m).

2.1.3 Intermediate Grid (Grid 3)

The third nested grid covers Chatham Sound, the Prince Rupert Harbour waterway and surrounding passes and inlets (Figure 2.3). This grid is of considerable importance since it determines the periods, Q-factor (attenuation rate) and other parameters of the eigen-oscillations set up in the harbour by incoming tsunami waves. Model grid cells were created using the 50-m pre-gridded CHS data provided as part of this study. The gridded data were subsequently re-interpolated from the original local UTM projection to a geographical coordinate system (NAD83 standard) with a rectangular grid cell size of 3 arc-seconds by 1.8 arc-seconds (approximately 54 m by 56 m) in the east-west and north-south directions, respectively.

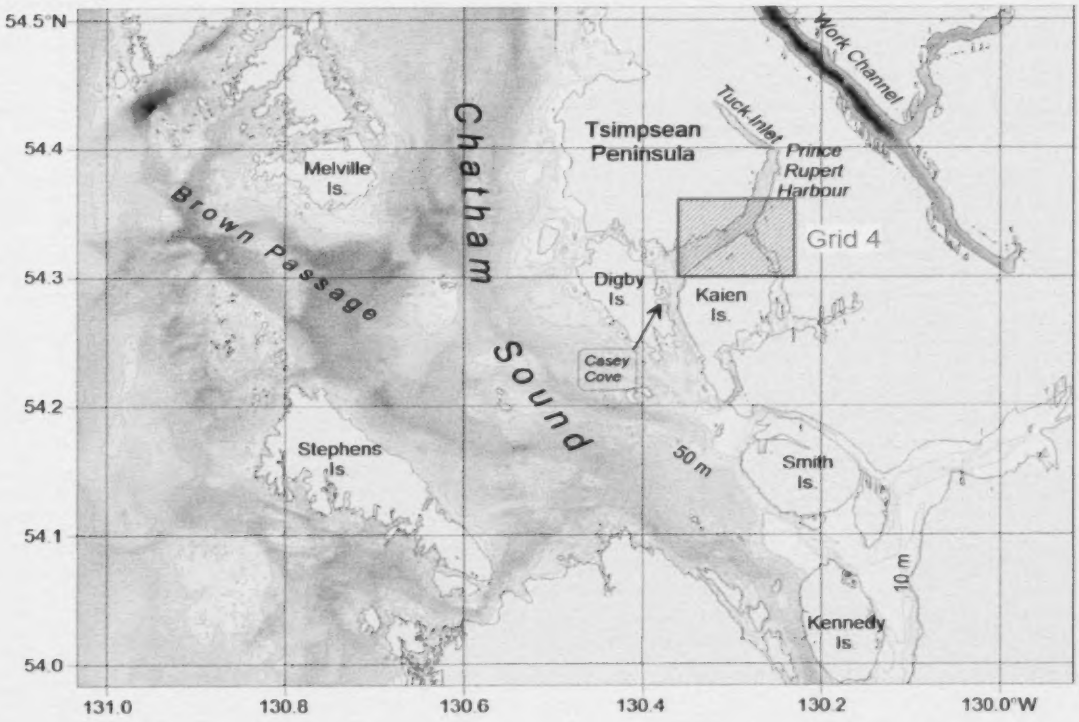

Figure 2.3. Coastal region covered by Grid 3, including Chatham Sound, Brown Passage and Prince Rupert Harbour. The grid scale for this region is approximately 54 m by 56 m. The insert shows the boundaries and location of the third nested grid (Grid 4) covering Seal Cove. Depths are in metres (m).

2.1.4 Final Grid (Grid 4)

The final (fourth) numerical grid has the highest spatial resolution and covers coastal areas near the DFO Coast Guard facilities (Figure 2.4). The grid has been adjusted for the site reconstruction and is designed specifically for estimations of tsunami inundation and tsunami-induced currents in the vicinity of the Coast Guard facilities. A Kriging algorithm (Matheron, 1963) was used to create the grid from the original, irregularly spaced CHS bathymetric and coastline data from analogue charts. Details on Kriging can be found in Thomson and Emery (2014). The grid (x, y) scale is approximately 11 m by 9 m.

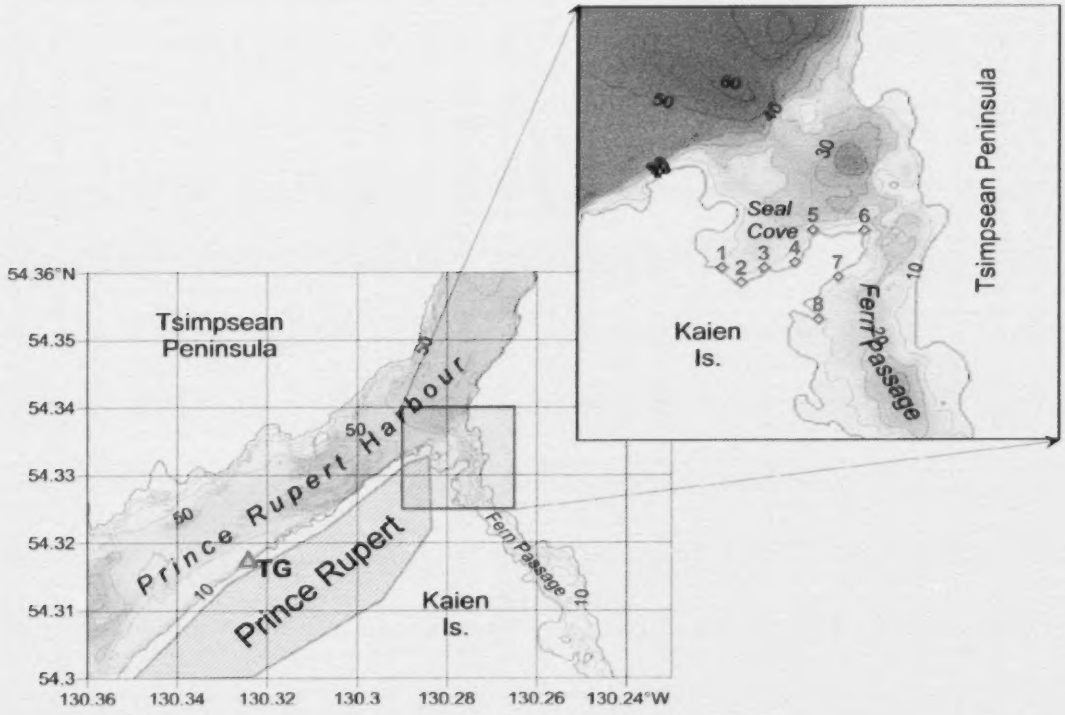

Figure 2.4. The region covered by Grid 4. The fine-scale bathymetric grid has adjusted topography for the region of Prince Rupert and Seal Cove, and has a grid (*x*, *y*) scale of approximately 11 m by 9 m. Also shown are the location of the tide gauge (TG) and the sites at Seal Cove (1-8) for which we have simulated tsunami wave records. Depths are in metres (m).

2.2 MODEL REFERENCE LEVELS

Simulations are generally conducted for tsunami arrival times that coincide with times of mean higher high water (MHHW), as per recommendations for computation of tsunami inundation in the United States (National Tsunami Hazard Mapping Program, 2010; Suleimani et al., 2013). Accordingly, maps of maximum tsunami wave height and current speed presented in this report are referenced to the MHHW mark rather than to the mean tide or to a geodetic reference.

MHHW is used as a reference level for all modelling results. For the Prince Rupert tide gauge, MHHW is 2.32 m above Mean Sea Level (MSL). Similarly, for the Casey Cove tide gauge, located on Digby Island (see Figure 2.3), MHHW is 2.32 m above MSL (Table 2). Based on these measurements, a common reference value of 2.3 m is applied throughout the Prince Rupert region for the tsunami modelling.

Table 2. Chart datum values for stations 9350 and 9354 provided by the CHS. Latitude and longitude are in degrees and minutes. Higher High Water (HHW) is defined in two ways: using all tidal values (Mean) and using only the highest tides (Large). Z_0 is the mean tidal constituent obtained by harmonic analysis of the tidal series.

Tide gauge ID	Name	Latitude (°N)		Longitude (°W)		HHW (m)		MSL (m)
		Deg	Min	Deg	Min	Mean	Large	Z_0
9350	Casey Cove	54	16	130	22	6.13	7.34	3.81
9354	Prince Rupert	54	19	130	19	6.16	7.46	3.849

2.3 THE TSUNAMI SOURCE DISTRIBUTION

Numerical simulation of an Alaska-type 1964 tsunami presented here is based on the newly revised (Suleimani et al., 2013) coseismic slip distribution for the 1964 rupture derived from the model of Suito and Freymueller (2009). The latter is a three-dimensional viscoelastic model, in combination with an after-slip model, which uses realistic geometry with a shallow-dipping elastic slab to describe the post-seismic deformation that followed the 1964 earthquake. The authors applied the inversion-based model by Johnson et al. (1996) as a basis for their coseismic slip model, adjusting it to the new geometry and critically reinterpreting the coseismic data.

Suleimani (2011) used results of the near-field modelling of the 1964 tsunami to constrain the amount of slip placed on intraplate splay faults, and to evaluate the extent of the Patton Bay fault. The revised model included a contribution of coseismic horizontal displacements to the initial tsunami wave field through the component of ocean surface uplift due to horizontal motion of the steep ocean bottom slopes. Numerical tsunami simulations revealed that including the deformation due to horizontal displacements in the source function resulted in an increase in the far-field tsunami amplitudes. The coseismic vertical deformation resulting is shown in Figure 2.5.

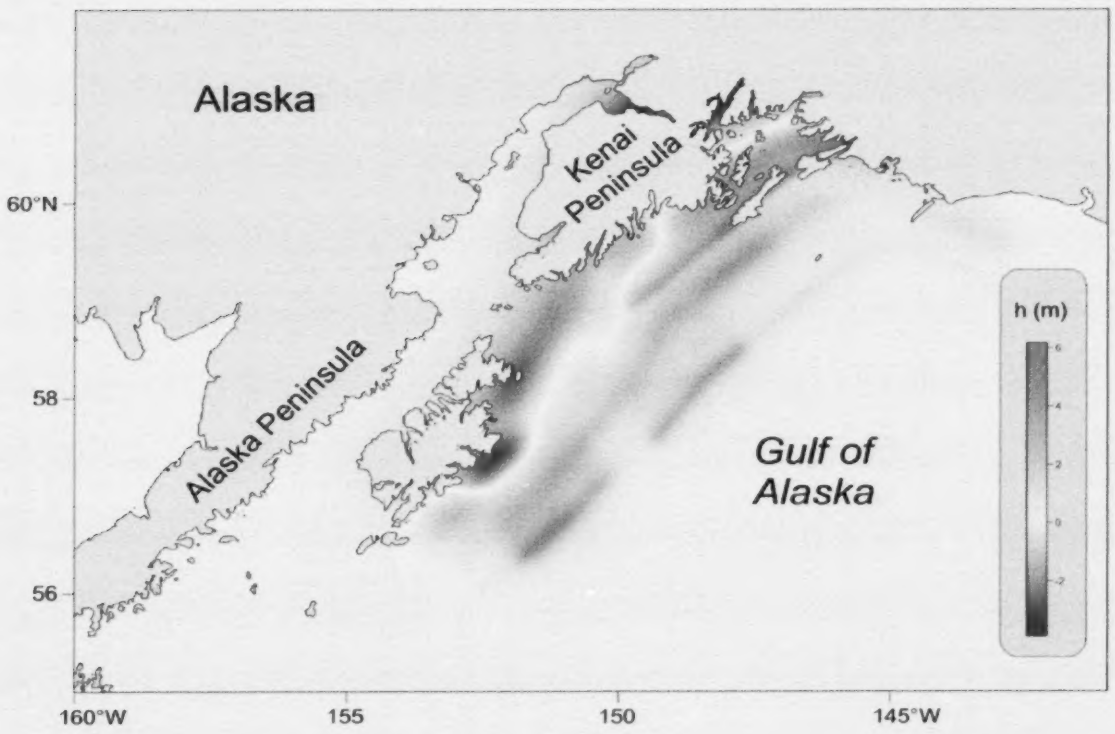

Figure 2.5. Seafloor vertical displacement (m) at the source region for the March 1964 Alaska tsunami (Suleimani *et al.*, 2013). Seafloor displacements range from roughly -3 m (blue) to +6 m (red).

This page is left intentionally blank

3 RESULTS

3.1 COMPARISON OF MODELLED TSUNAMI WAVES WITH OBSERVED WAVES AT THE PRINCE RUPERT TIDE GAUGE

To verify the tsunami model results, we compared the modelled results with the record of the Alaska 1964 tsunami at the Prince Rupert tide gauge. The analogue gauge record of the tsunami was digitized and the tides carefully removed using tidal analysis programs (cf. Thomson and Emery, 2014). Comparisons of the observed and modelled tsunami waves are presented in Figure 3.1 and Table 3. The modelled record closely matches the observed record and the wave forms are nearly identical. Moreover, because of improved tsunami source region distribution and much more accurate and detailed bathymetry used in this study, the modelled waves fit the observed waves much better than in previously published numerical results (Dunbar *et al.*, 1991).

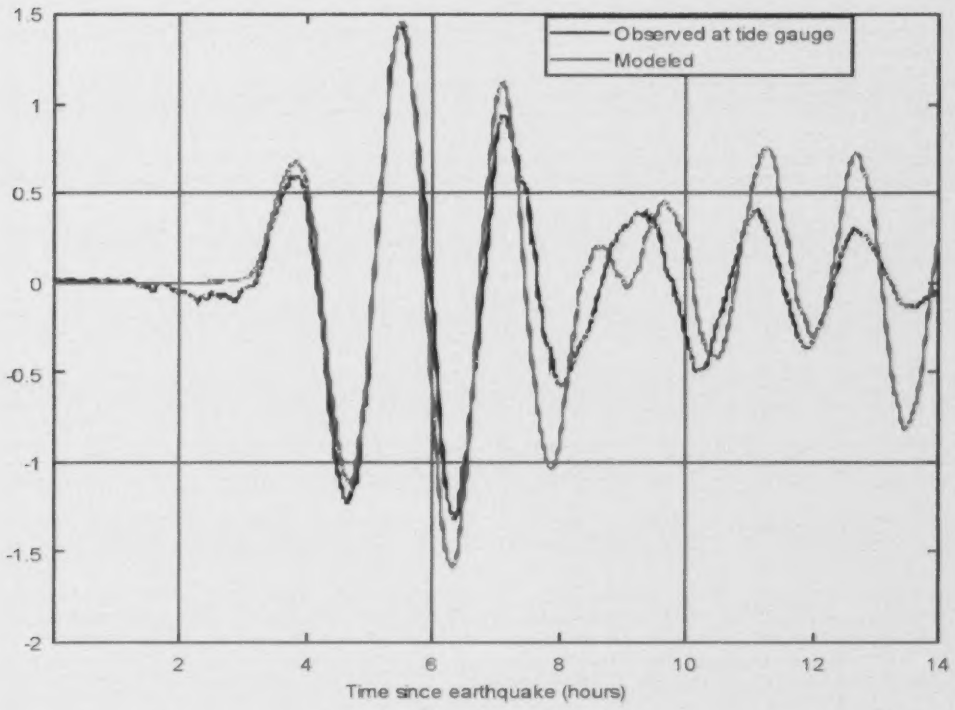

Figure 3.1. Observed versus modelled wave records for the March 1964 Alaska tsunami for the Prince Rupert tide gauge site.

Table 3. Statistical properties of modelled and observed tsunami waves at the Prince Rupert tide gauge location for the March 1964 tsunami source region. Wave heights are in metres and travel times in hours (h) and minutes (min).

	First wave		Maximum crest		Maximum trough	
	Amplitude (m)	Travel time (min)	Amplitude (m)	Travel time	Amplitude (m)	Travel time
Modelled	0.71	3h 51	1.48	5h 35 min	-1.55	6h 24 min
Observed	0.59	3h 46	1.43	5h 28 min	-1.31	6h 20 min

3.2 MAXIMUM TSUNAMI HEIGHTS

The computed distributions of wave height maxima for a future Alaska-type tsunami, for Grids 1-3, are presented in Figures 3.2-3.4. Figure 3.2 shows the "rays" of maximum tsunami wave heights for in the entire northeast Pacific. While tsunami wave-height maxima are located in Prince Williams Sound (the source area), considerable tsunami energy is radiated to the southeast toward the British Columbia and Californian coasts. In Southern Alaska and British Columbia, the most affected coastal zones are those exposed to the open ocean, such as the west coasts of Vancouver Island and Haida Gwaii. In more protected areas such as Hecate Strait, the computed tsunami wave amplitudes are markedly smaller (Figure 3.3; Grid 2).

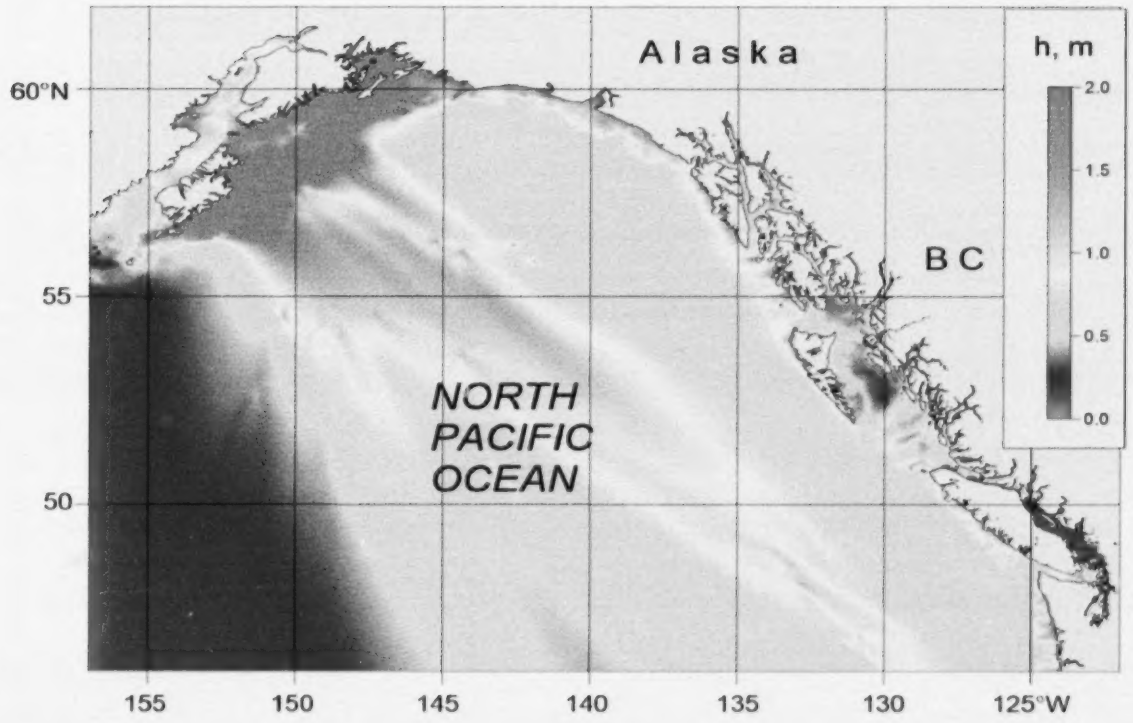

Figure 3.2. Distribution of maximum tsunami wave heights (h, in metres) for Grid 1 of the nested-grid model for waves associated with the 1964 Alaska tsunami.

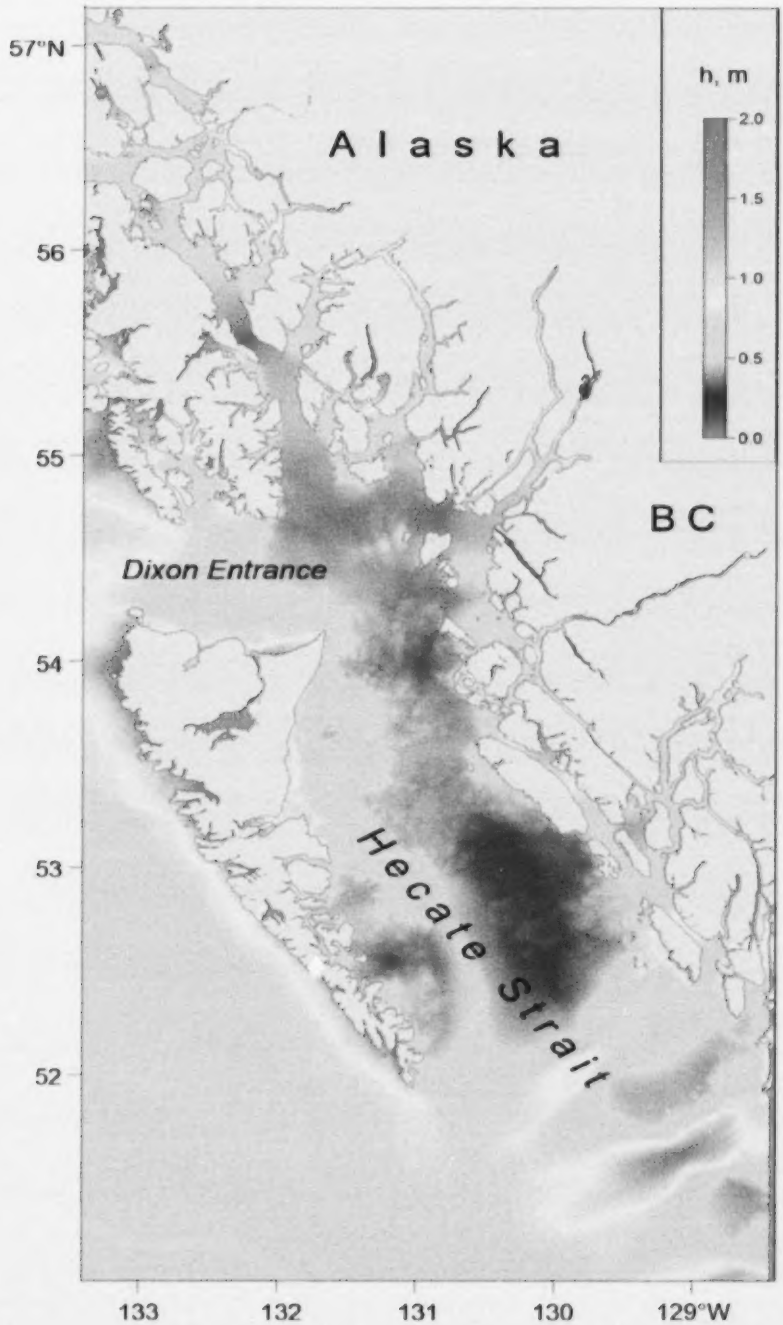

Figure 3.3. Distribution of maximum tsunami wave heights (metres) for Grid 2 of the nested-grid model for waves associated with an Alaska-type 1964 tsunami.

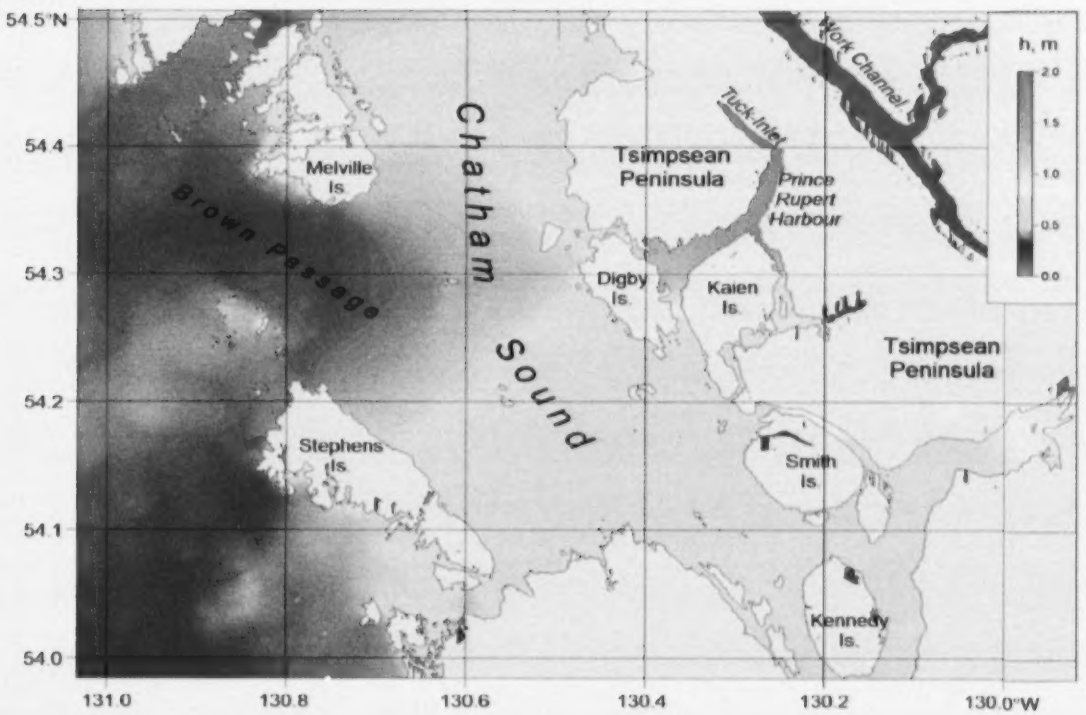

Figure 3.4. Distribution of maximum tsunami wave heights (metres) for Grid 3 of the nested-grid model for waves associated with an Alaska-type 1964 tsunami.

Results for the finer resolution grids (Grids 3 and 4) demonstrate the considerable spatial variability in the incoming tsunami wave heights for the study region. Figure 3.4 shows the distribution of the tsunami wave heights in Chatham Sound and neighbouring areas for Grid 3. The wave amplitudes increase toward the shoreline, especially in Prince Rupert Harbour and Tuck Inlet, where the wave amplitudes are 4-5 times higher than in the eastern part of Chatham Sound and Brown Passage. The pronounced increase in tsunami wave heights in the Prince Rupert Harbour basin is related to resonance amplification of the tsunami waves whereby the period (~ 2 hours) of the incoming waves is close to the period of the eigen-oscillations of the basin.

3.3 DETAILED RESULTS FOR SEAL COVE: VARIATIONS IN SEA LEVEL AND TSUNAMI-INDUCED CURRENTS

Figure 3.5 presents a high-resolution map of the maximum tsunami heights in Prince Rupert and vicinity for numerical Grid 4. As the figure indicates, amplitudes of the tsunami waves gradually increase along Prince Rupert Harbour, from 1.3 m in south-west to 1.7 m at northeast end of the grid. In Seal Cove, the tsunami wave maxima are distributed almost uniformly, with a value of around 1.55 m. In Fern Passage, just south of Seal Cove, the tsunami wave amplitudes decrease to 1.2 to 1.3 m.

Figure 3.6 shows the distribution of the tsunami current maxima. For Seal Cove, the tsunami-induced currents are weak and do not exceed 0.5 m/s (1 knot). However, in nearby Fern Passage, the tsunami currents are much stronger, with currents in the middle of Fern Passage reaching speeds of 2.5 m/s (5 knots).

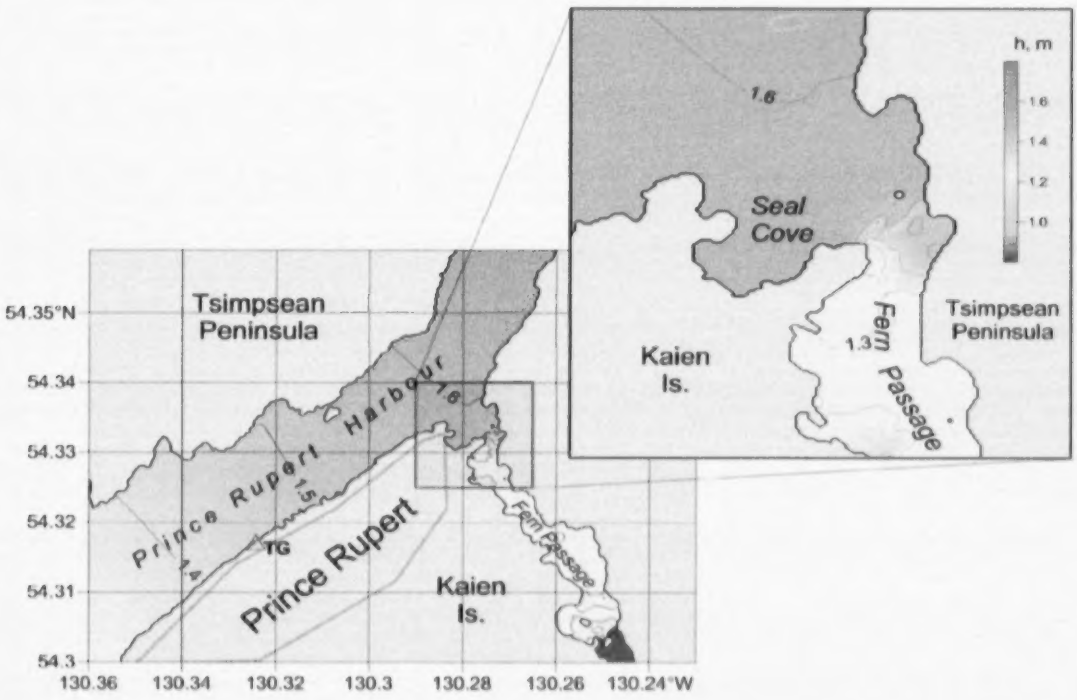

Figure 3.5. Distribution of maximum tsunami wave heights (metres) for Grid 4 of the nested-grid model for waves associated with an Alaska-type 1964 tsunami. The insert shows an enlarged segment of the Seal Cove area.

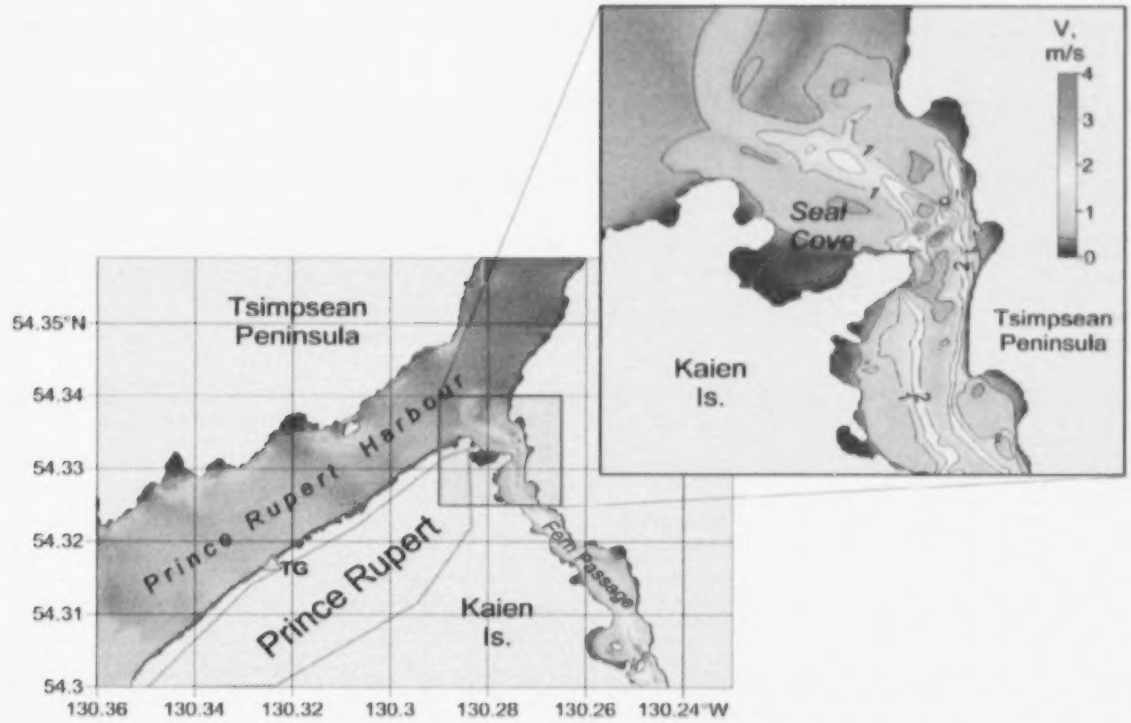

Figure 3.6. Distribution of the maximum of modelled tsunami- generated currents (in m/s) for Grid 4. The insert shows an enlarged segment of the Seal Cove area.

Simulated tsunami-generated sea level variability at specific sites on the north coast, around Seal Cove and the mouth of Fern Passage (Figure 3.4), is shown in Figures 3.7 to 3.8. Tsunami waves arriving at Seal Cove from this simulated event are 5-10% higher than those at the Prince Rupert tide gauge (see Figure 3.1) but generally very close to those for Prince Rupert Harbour. The wave amplitudes at Sites 1, 2, 3 and 4 are very similar and hence only Site 4 results are shown (Figure 3.7). The simulated wave heights for Site 5 (Figure 3.8) are also similar to results for Sites 1, 2, 3 and 4, while tsunami wave simulations at Sites 6, 7, and 8 are a bit lower. Generally, all records are very similar, indicating that the Seal Cove basin is too small to amplify the low frequency (period about 2 hours) of the incoming waves generated during a future 1964-type tsunami.

The records of wave-generated currents are presented in Figures 3.9 to 3.12. Results reveal that currents at sites 1 to 4 are very weak (Figure 3.9 and3.10). Typically, they are below 5 cm/s, except for the eastward velocity at Site 3, where the current reaches 15 cm/s. At

Sites 5 to 8, the currents are much stronger than at Sites 1 to 4. Especially strong currents of up to 200 cm/s, equivalent to 2 m/s, occur at Site 6, located at the end of Seal Cove peninsula. We further note that the current speeds are asymmetrical in direction, which may be related to nonlinear effects. Current speeds vary non-uniformly over the area.

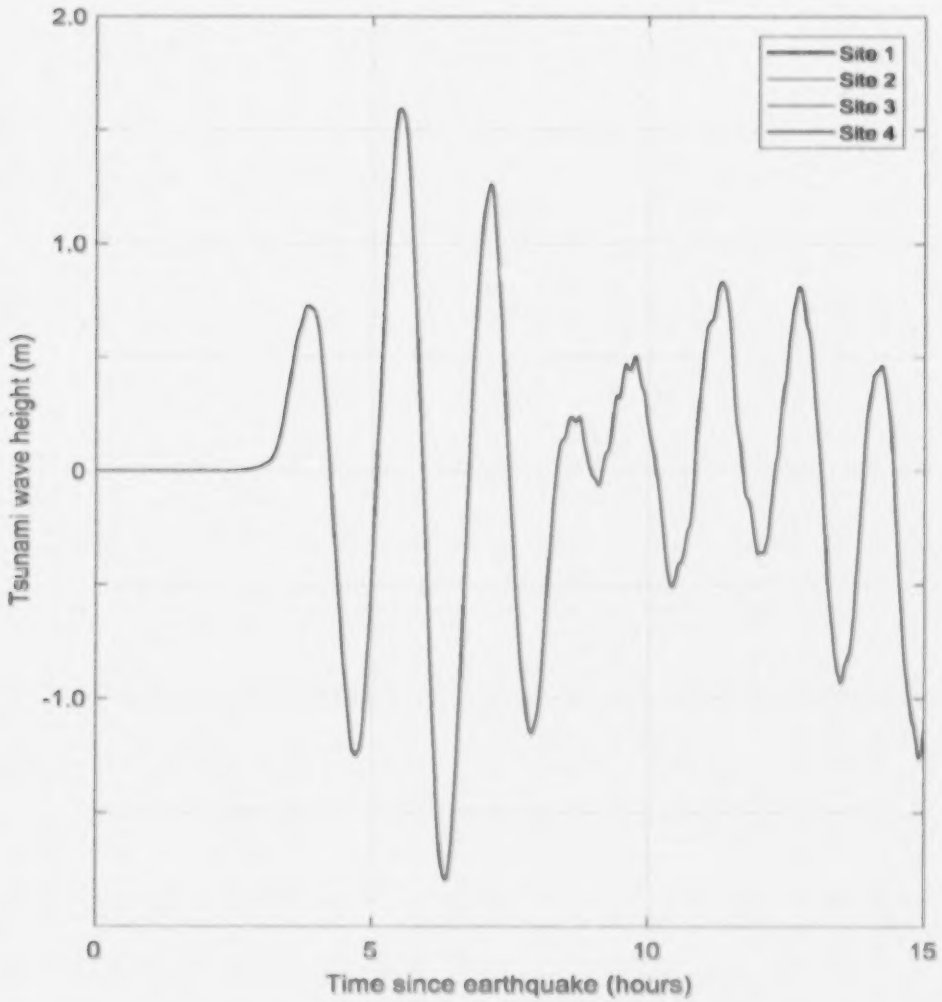

Figure 3.7. Site 4 simulated records of water level variations for an Alaska-type 1964 tsunami. Only the records for Site 4 are presented, as those for the other three sites noted in the legend are almost identical.

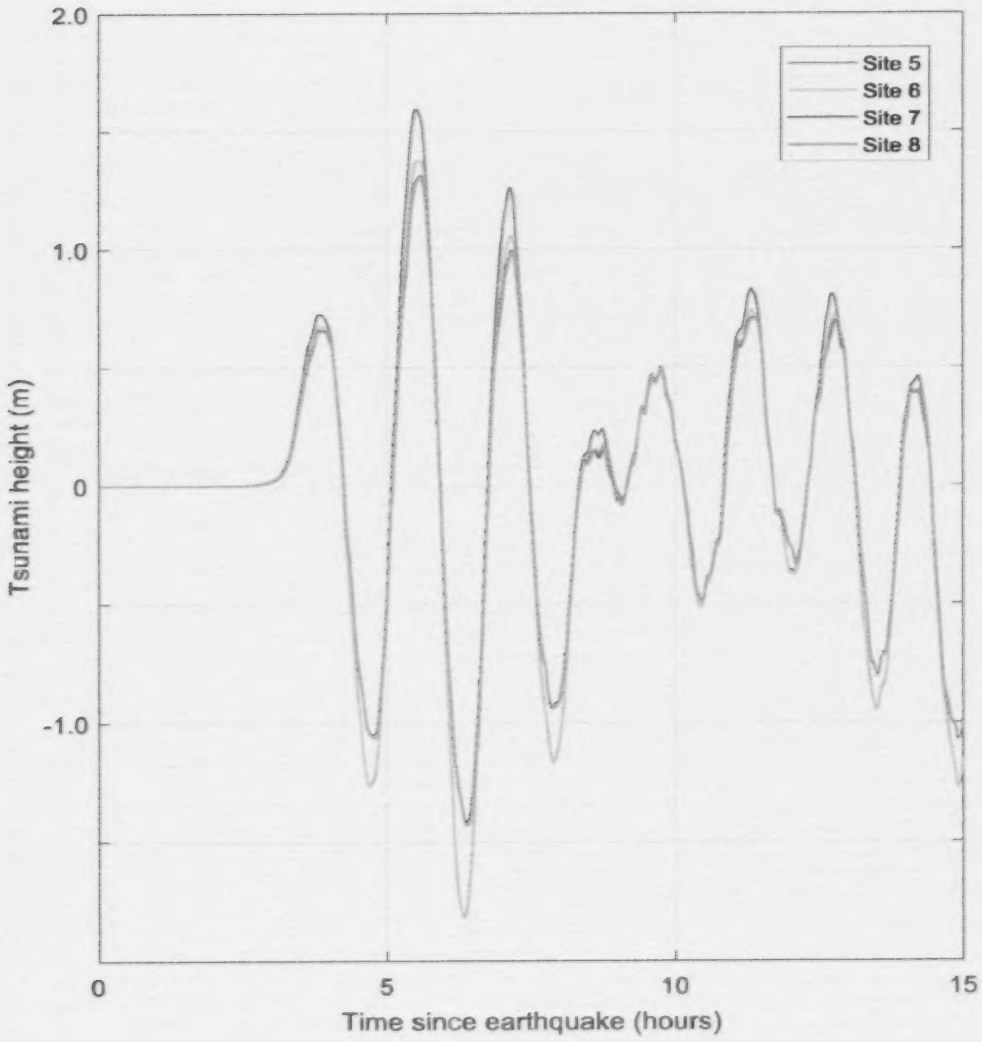

Figure 3.8. Simulated records of water level variations for an Alaska-type 1964 tsunami at Sites 5, 6, 7 and 8 (See Figure 2.4 for the site locations).

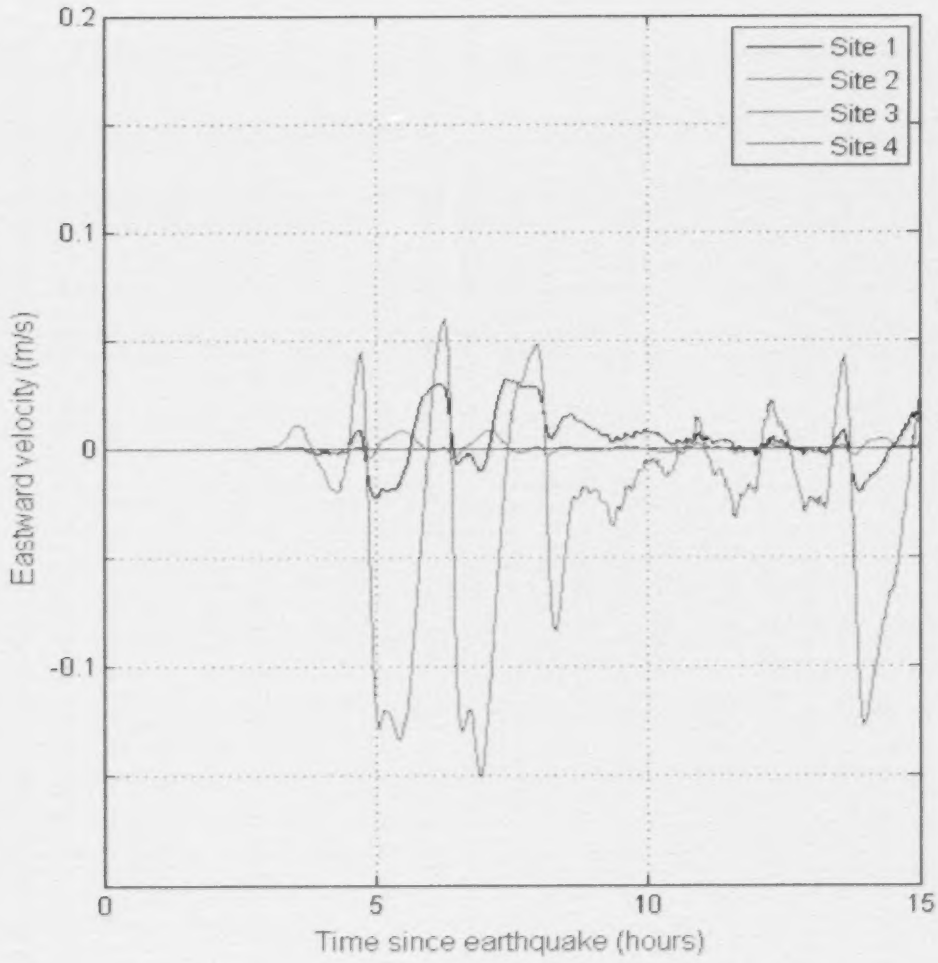

Figure 3.9. Simulated records of the eastward current velocity for an Alaska-type 1964 tsunami at Sites 1, 2, 3 and 4 (See Figure 2.4 for the locations).

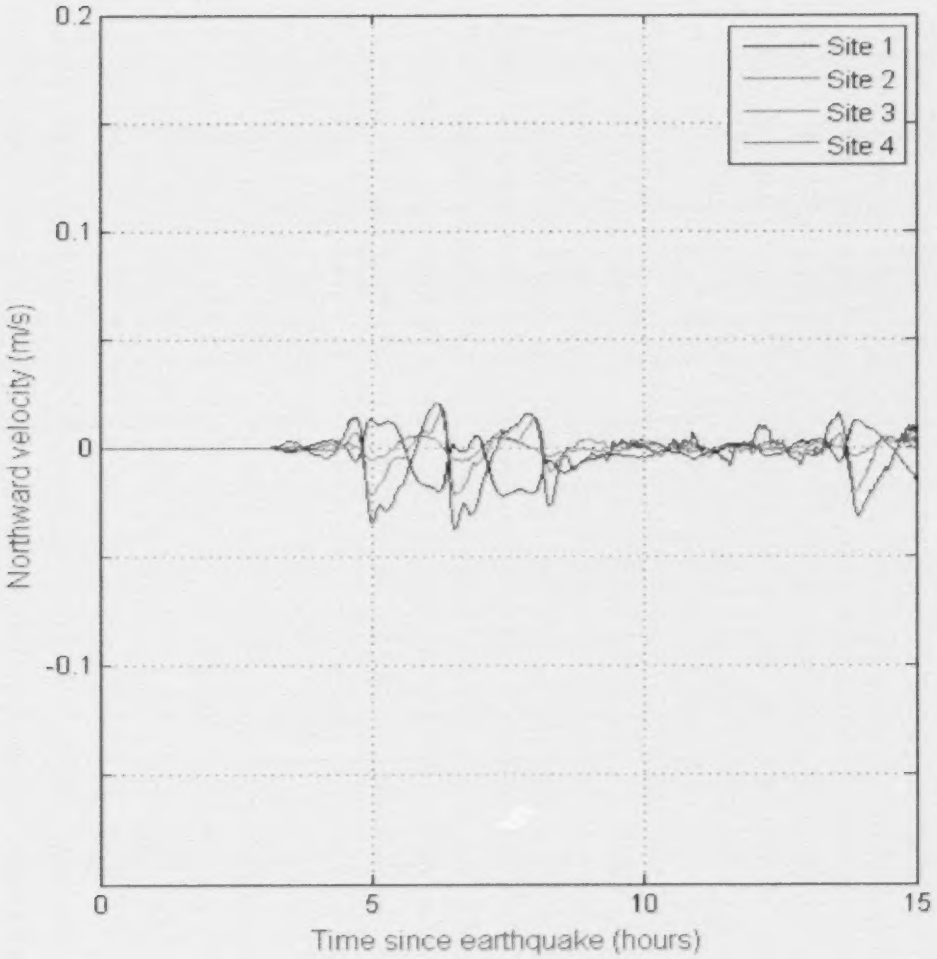

Figure 3.10. Simulated records of the northward component of current velocity for an Alaska-type 1964 tsunami at Sites 1, 2, 3 and 4 (See Figure 2.4 for the locations).

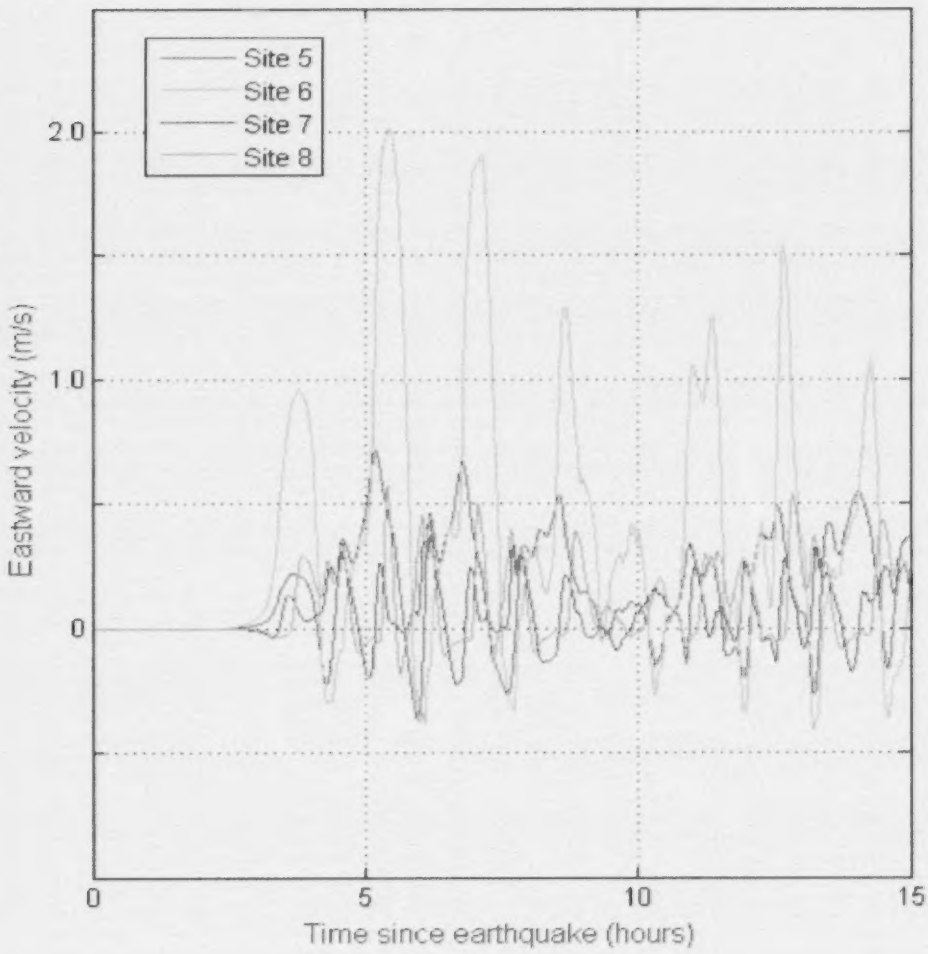

Figure 3.11. Simulated records of the eastward component of current velocity for an Alaska-type 1964 tsunami at Sites 5, 6, 7 and 8 (See Figure 2.4 for the locations).

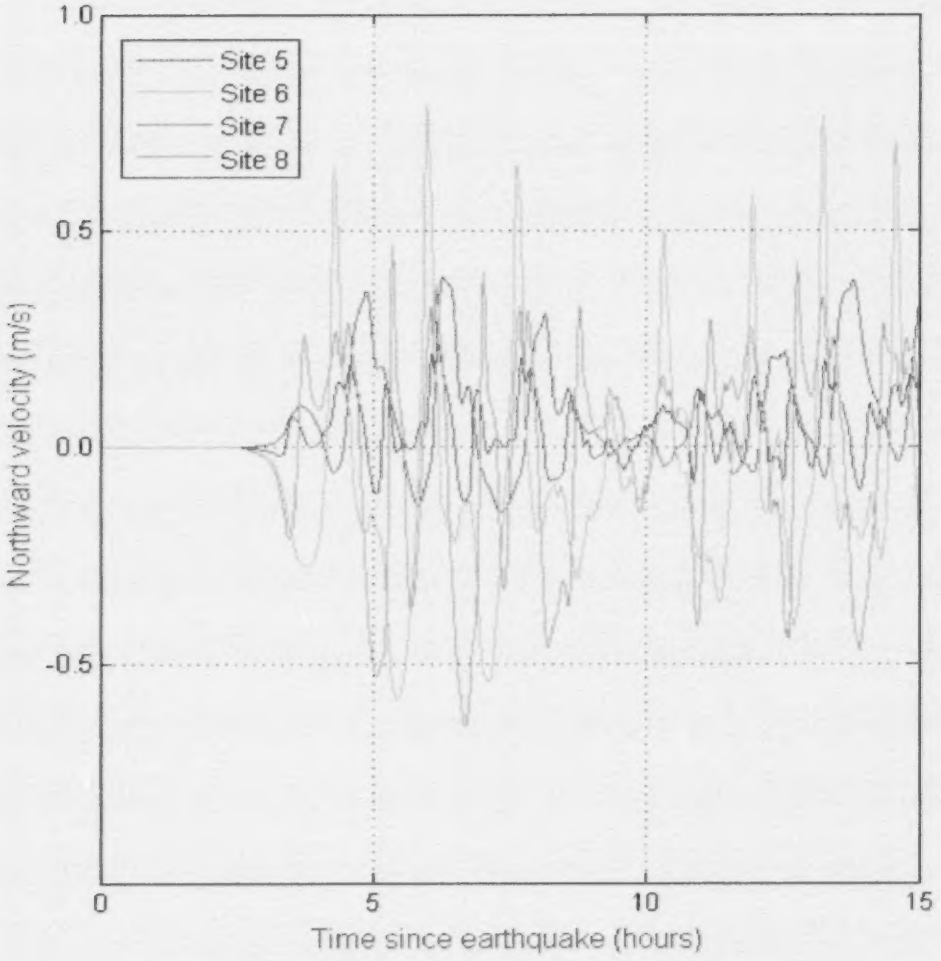

Figure 3.12. Simulated records of the northward component of current velocity for an Alaska-type 1964 tsunami at Sites 5, 6, 7 and 8 (See Figure 2.4 for the locations).

This page is left intentionally blank

4 CONCLUSIONS

A high-resolution nested-grid tsunami model was used to simulate tsunami waves and wave-induced currents that will be generated in Seal Cove by an earthquake and tsunami similar to that of the 1964 Alaska event. The model used an advanced tsunami source distribution and high-resolution bathymetry for the area of interest. The major results of the numerical modelling are:

- Tsunami wave heights in Seal Cove will reach 1.55 m above the tidal level at the time of the event; the second wave will be the highest wave;
- The second wave crest will arrive approximately 100 minutes after the first wave crest. Tsunami wave periods range from 70 to 105 minutes;
- Tsunami wave amplitudes will be nearly uniform throughout Seal Cove;
- Tsunami-induced currents in Seal Cove will be weak (< 0.5 m/s);
- Tsunami-induced currents in neighbouring Fern Passage will be quite strong and reach speeds of approximately 2.5 m/s;
- Because the details of future possible tsunamis remain unknown in many aspects, we recommend use of a safety factor of 50% to be added to predicted tsunami amplitudes during a 1964 Alaska-type event. In this case, the safety water level for Seal Cove should be at least 2.28 m above Mean Higher High Water (MHHW), or 4.6 m above Mean Sea Level (MSL).

More detailed predictions on the landward extent of tsunami wave run-up and inundation in the Seal Cove region will require more advanced numerical simulations, which permit wetting and drying of the land. The model should be able work with strong nonlinearity and friction, and allow for a discontinuity between wet and dry numerical domains. Such studies also require detailed coastal elevation data and Lidar bathymetry along the shoreline.

This page is left intentionally blank

5 ACKNOWLEDGEMENTS

The authors gratefully thank Peter Wills and Denny Sinnott of the Canadian Hydrographic Service for providing the bathymetric data and tide gauge records for this study. Alexander Rabinovich and Maxim Krassovski of the Institute of Ocean Sciences assisted with the data processing and numerical grid formulation, and Elena Suleimani at the University of Alaska at Fairbanks provided the latest source model for the Alaska 1964-type earthquake and tsunami. Lastly, we thank Alison Scoon for helping transform the original report into a formal technical report.

This page is left intentionally blank

6 REFERENCES

Anderson, P. S. and Gow, G. A. (2004), Tsunamis and Coastal Communities in British Columbia: An Assessment of the B.C. Tsunami Warning System and Related Risk Reduction Practices.75xii pp. (Public Safety and Emergency Preparedness Canada, Ottawa, 2004).

Becker, J. J., D. T. Sandwell, W. H. F. Smith, J. Braud, B. Binder, J. Depner, D. Fabre, J. Factor, S. Ingalls, S-H. Kim, R. Ladner, K. Marks, S. Nelson, A. Pharaoh, R. Trimmer, J. Von Rosenberg, G. Wallace, P. Weatherall. (2009), Global Bathymetry and Elevation Data at 30 Arc Seconds Resolution: SRTM30_PLUS, Marine Geodesy, 32:4, 355-371, DOI: 10.1080/01490410903297766

Clague, J. J. (2001), Tsunamis. In A Synthesis of Geological Hazards in Canada (ed. G.R. Brooks) Geol. Surv. Canada, Bull. 548, 27–42.

Caldwell, R.J., Taylor, L.A., Eakins, B.W., Carignan, K.S., and Collins, S.V. (2012). Digital elevation models of Juneau and Southeast Alaska—Procedures, data sources and analysis: National Geophysical Data Center, NOAA Technical Memorandum NESDIS NGDC-53, 66 p.

Clague, J. J. (2001), Tsunamis. In A Synthesis of Geological Hazards in Canada (ed. G.R. Brooks) Geol. Surv. Canada, Bull. 548, 27–42.

Clague, J.J., Munro, A., and Murty, T.S. (2003), Tsunami hazard and risk in Canada, Natural Hazards 28 (2-3), 433-461.

Dunbar, D., LeBlond, P., and Murty, T.S. (1991). Evaluation of tsunami amplitudes for the Pacific coast of Canada. Prog. Oceanogr. 26, 115-177.

Fine, I.V., Cherniawsky, J., Rabinovich, A. and Stevenson, F. (2008) Numerical Modeling and Observations of Tsunami Waves in Alberni Inlet and Barkley Sound, British Columbia. In: Cummins, P.R., Satake, K., Kong, L.S.L. (eds) Tsunami Science Four Years after the 2004 Indian Ocean Tsunami. Pageoph Topical Volumes. Birkhäuser Basel.

Imamura, F., Shuto, N., and Goto, C. (1988). Numerical simulation of the transoceanic propagation of tsunamis. Paper presented at the Sixth Congress of the Asian and Pacific Regional Division. Int. Assoc. Hydraul. Res., Kyoto, Japan. vol. IV, p. 265-272.

Imamura, F., Yalciner, A. C. and Ozyurt, G. (2006). Tsunami modelling manual (TUNAMI model), 2006. http://www.tsunami.civil.tohoku.ac.jp/hokusai3/J/ projects/manual-ver-3.1.pdf.

Johnson, J. M., Satake, K., Holdahl, S. R., and Sauber, J. (1996). The 1964 Prince William Sound earthquake— Joint inversion of tsunami waveforms and geodetic data. J. Geophys. Res., 101, no. B1, p. 523–532.

Lander, J.F. (1996). Tsunamis Affecting Alaska, 1737-1996. Boulder, CO: U.S. Department of Commerce.

Liu, P. L.-F., Woo, S-B. and Cho, Y-S. (1998). Computer programs for tsunami propagation and inundation. Technical report, Cornell University.

Matheron, G. (1963). Principles of geostatistics. Economic Geology, 58, pp 1246–1266.

Myers, E.P. and Baptista, A.M. Analysis of Factors Influencing Simulations of the 1993 Hokkaido Nansei-Oki and 1964 Alaska Tsunamis. Natural Hazards (2001) 23: 1. https://doi.org/10.1023/A:1008150210289.

National Tsunami Hazard Mapping Program (NTHMP) (2010). Guidelines and best practices for tsunami inundation modeling for evacuation planning. NTHMP Mapping & Modeling Subcommittee, NOAA, USA.

Nikolsky, D.J., Suleimani, E.N., Haeusseller, P.J., Ryan, H.F., Kohler, R.D., Combellick, R.A. and Hansen, R.A. (2013). Tsunami Inundation maps of Port Valdez, Alaska. State of Alaska, Department of Natural Resources, Division of Geological & Geophysical Surveys.

NOAA (2017). British Columbia, 3 arc-second MSL DEM. https://www.ngdc.noaa.gov/dem/

squareCellGrid/download/4956. Last access on 11.10.2017.

Spaeth, M. G., and Berkman, S. C. (1967). The tsunami of March 28, 1964, as recorded at tide stations. Coast and Geod. Survey Techn. Bull. 33, US Department of Commerce, 86 p.

Suito, H., and Freymueller, J. T. (2009). A viscoelastic and afterslip post seismic model for the 1964 Alaska earthquake. J. Geophys. Res., 114, B11404, doi: 10.1029/ 2008JB005954.

Stephenson, F.E., Rabinovich, A.B., Solovieva, O.N., Kulikov, E.A. and Yakovenko, O.I. (2007). Catalogue of tsunamis, British Columbia, Canada: 1700-2007. Preprint. P.P. Shirshov Inst. Oceanology, Moscow, 134 p.

Suleimani, E. N. (2011). Numerical studies of tectonic and landslide-generated tsunamis caused by the 1964 Great Alaska Earthquake. Fairbanks, Alaska, University of Alaska Fairbanks, Ph.D. dissertation, 181 p.

Suleimani, E. N., Nicolsky, D. J., and Koehler, R. D. (2013). Tsunami Inundation Maps of Sitka, Alaska. Report of Investigations 2013-3, State of Alaska, Department of Natural Resources, Division of Geological and Geophysical Surveys, Fairbanks, AK, 76 p., 1 sheet, scale 1:250,000. doi: 10.14509/26671.

Thomson, R. E. and Emery, W. J. (2014). Data Analysis Methods in Physical Oceanography: 3rd Edition. Elsevier Science, Amsterdam, London, New York (August 2014), 716 p.

Wang, X. (2009). User Manual for COMCOT Version 1.7. http://ceeserver.cee.cornell.edu/pll-group/doc/COMCOT_User_Manual_v1_7.pdf.